The Impact of Cask Wake on Materials Released From a Type B Cask

Christopher Clutz and Ruth Weiner

Sandia National Laboratories, PO Box 5800, Ambuquerque, NM 87185; cclutz@sandia.gov
Boston Government Services105 Mitchell Road, Oak Ridge, TN 37830, rweiner@bgs-llc.com

If a Type B cask carrying spent nuclear fuel is in a traffic accident, some radioactive material could be released to the environment. Dispersion of this material is usually modeled as Gaussian dispersion which is inapplicable closer than about 30 meters to the source of the released material. This document describes an initial attempt to model dispersion from the source out to 20 to 30 meters from the source, in the "near field." Preliminary results of this model suggest that less radioactivity is dispersed when there is a release from the cask than has been postulated in other studies. However, there is also a strong indication that radioactive material would be trapped near the cask by the downwash on the downwind side of the cask.

I. INTRODUCTION

RADTRAN is an internationally accepted program and code for calculating the risks of transporting radioactive materials. The first versions of the program, RADTRAN I and II, were developed for NUREG-0170[1], the first environmental statement on transportation of radioactive materials. RADTRAN calculates individual and collective doses for a number of different receptors. Workers and inspectors who work in a significant radiation field generally carry personal dosimeters and the doses are maintained as low as reasonably achievable/

However, a complete model of the doses from an accident in which radioactive material is released should include both the doses to the resident public along the route and to receptors very near the package or cask containing radioactive material – the "near field." This project was initiated as a dose model for the near field. As the modeling progressed, the need for a distinct model for the near field was obviated. The action of the wake over the cask appeared to trap the released material at approximately ground level close to the cask, resulting in a decrease in the amount of released material available for dispersal in the far field. Incorporation of this phenomenon into RADTRAN is straightforward: the decrease in dispersible material can be coupled with the wind velocity.

I.1 Radiation Dose When There Is No Release of Radioactive Material

Type B casks carry very radioactive material, like spent nuclear fuel, and are therefore sufficiently robust that they can withstand severe traffic accidents[2]. However, there will be some external radiation from the cask during ransportation.[3]

I.2 Radiation Dose When Radioactive Material Is Released

Radiation doses from accidental releases of radioactive material are usually modeled using a Gaussian dispersion model. This model is exceedingly inaccurate closer to the source than about 20-30 meter. Equation 1 is the general Gaussian puff equation:

$$\frac{CHI}{Q} = \frac{1}{2\pi^{3/2} u \sigma_y \sigma_z} \exp\left(\frac{-y^2}{2\sigma_y^2}\right) \exp\left(\frac{-H^2}{2\sigma_z^2}\right) \quad (1)$$

CHI (the Greek X) = air radioactivity concentration
Q = radioactivity released
$\sigma_y(x)$, $\sigma_z(x)$ – meteorological constants that define the Gaussian
u = wind speed
H = height of the radioactive release above ground

The meteorological constants σ_y and, σ_z are functions of x, the downwind distance from the location of the radioactivity release. As that distance

x approaches zero, the dilution CHI/Q becomes infinitely large, so that the Gaussian is inapplicable.
As x approaches zero, the dilution CHI/Q becomes infinitely large, so that the Gaussian is inapplicable.

The original focus of radioactive material transportation risk was the risk to the public along the transportation route[1] who would be several tens of meters from the vehicle in the event of an accident. As the program developed, the need for a model to estimate doses to emergency responders, and other workers who might be near the cask became evident. In the case of a transportation accident involving a spent fuel transport, members of the public may be within a few meters of the cask. Moreover, some emergency responders may not be carrying dosimeters and some rails or railyard crew may not have dosimeters. Longshoremen who load and unload spent fuel casks may not have dosimeters because the country in which they work may not require them. Policemen at state inspection stations rarely wear dosimeters. This project was focused on designing a model for estimating these primarily occupational doses.

II TWO-DIMENSIONAL, LOCAL POLLUTANT TRANSPORT BY CASK DEPRESSURIZATION IN THE PRESENCE OF WIND

II.1 Factors Affecting the Dose Model

The dose model described in this report considers radionuclide emission from a damaged transportation cask and the potential effect on dispersion of the material released from the cask. The radionuclides emitted are assumed to all have diameter of the order of one micron, to be spherical, and to be passive test particles in the flow field. The model is a fluid dynamics model, because both the ambient wind and the gases and aerosol-sized particles emitted can be treated as a fluid. Behavior of the released radioactive material depends on these factors.

1. The pressure differential between the pressure inside the cask and the ambient atmospheric pressure drives the release. The pressure in the cask, which is due to both the internal pressure of the spent fuel rods and to the temperature differential between the cask interior and the ambient temperature, is the force that drives the release. The internal pressure of the cask at the beginning of the release is about five times the ambient atmospheric pressure. Although the pressure is equalized in a few seconds, the differential determines the initial shape of the released plume.
2. When the pressure in the cask and the ambient air pressure are equalized, the movement of the released plume changes.
3. Because the cask is a large object, it distorts the wind flow, resulting in turbulence on the downwind side of the cask and in the often-observed downwash effect[3], Downwash could result in trapping the released plume of radioactive material near the ground close to the cask, and could thus affect the concentration of radioactive material in the near field.

RADTRAN is a two-dimensional model, and the model considered here is also two-dimensional. The cross-sectional area of the cask is modeled as perpendicular to the wind direction and the length of the cask is not part of the model. The results of a three dimensional model may be quite different; and such a model should be tested experimentally before any conclusion regarding the effects on RADTRAN

II.2 Description Of The Model And Its Implementation

In RADTRAN[4] as in other codes whose capabilities include transport of pollutants, details of pollutant flow near the site of radioactive materials release are ignored or are treated in a rather *ad hoc* manner, for several reasons.

1. Atmospheric dispersion of radioactive materials has historically been modeled as dispersion of a Gaussian plume, but, as Equation (1) shows, this model would not be applicable at short distances downwind. The practical minimum distance for applying the Gaussian model is about 20 meters.
2. Atmospheric dispersion was first modeled in the 1960s[5] when computational fluid dynamics was in its infancy.
3. Individuals near the site would probably be emergency responders and would be wearing dosimeters, obviating, in part, the need for a model. Potentially important aspects of near field behavior are treated with insufficient detail. For example, estimate of the amount of material reaching the atmospheric transport (far field) domain are imprecise, and no information about local deposition and dispersion of pollutants can be provided.

In order to provide a better simulation, a near - field analysis must simulate the relevant physics, and the domain should include the region, surrounding the damaged cask, within which Gaussian models of atmospheric transport and dispersion are not applicable. The physical environment influencing pollutant dispersion consists of the thermal and mechanical conditions at the cask rupture site; a ground level ambient wind field; a vertical temperature gradient representing the atmospheric lapse rate; and mechanical and thermal (and possibly chemical) properties of the pollutant particles. A complete physical simulation of pollutant motion in the near field should take this environment as its starting point and track pollutant particles within a transient, three dimensional flow field, accounting for turbulence, buoyancy, and convective and conductive heat transfer. Such a simulation would require a transient, 3D solution of the Navier-Stokes equations and equations of thermal energy balance. Such a simulation is beyond the scope of this project.

The first step towards such a complete simulation is a series of transient, two dimensional simulations in which the pollutant is assumed to be aerosolized as one micron diameter spheres. Other physical processes are not simplified: buoyancy, heat transfer, and Navier-Stokes momentum transfer (including turbulence modeling) were all directly simulated, using ANSYS Fluent[6]**.**

Figure 1 shows the near field simulation domain. In all two-dimensional simulations, the amount of pollutant exiting the domain and entering into atmospheric transport is never more than 60 percent of the outgassed aerosol mass, as shown in Table 1. This is a significant departure from the traditional assumption that all of the aerosolized pollutant mass reaches the atmospheric transport domain, and shows the importance of detailed near field considerations in assessing consequences of severe transportation cask accidents

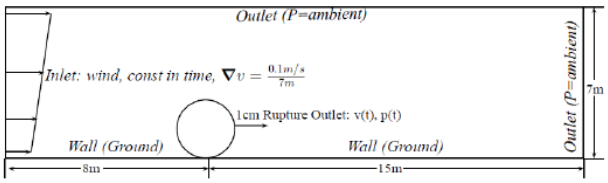

Fig. 1. Near field simulation domain

The code ANSYS[6] was used to model the air flow and particle release. Four two-dimensional computational fluid dynamics (CFD) simulations using ANSYS Fluent were performed using the geometry shown in Figure 1. The four simulations differed only in the strength of the ambient wind field surrounding the rail cask. The other conditions, applied to all four simulations, were:

1. The pollutant particles were treated using a dilute gas approximation, with full thermal interaction with the air. A temperature change of -0.1 deg. K was applied over the height of the domain show This change is consistent with the dry adiabatic atmospheric lapse rate[7].
2. Bluff body wake generation was induced geometrically, by putting a small re-entrant corner on the cask, located at θ=330 degrees, where θ is indicated on the cask cross section in Figure 1.
3. A change in the horizontal wind velocity of 0.1m/s with altitude upwind of the cask. This is to simulate the velocity gradient of the atmospheric boundary layer. Also, the ground surface upwind of the cask is assumed to be completely reflective, as would be the case for the atmospheric boundary layer very close to the ground.
4. Because of the radioactive decay heat generated by spent fuel, a temperature of 750 deg. K inside the cask, with an associated ideal gas pressure of 62 atm. (given a typical rail cask's free volume). The internal temperature represents an upper limit on that allowed by regulation[4].
4. A one cm. wide rupture in the cask, at a location facing directly downwind (3 o'clock on the cask in Figure 1). Because of this small rupture, the cask does not immediately reach mechanical equilibrium with the ambient air pressure (one atmosphere), but takes some time to depressurize. Initially, the flow from the 1 cm. rupture is choked so that the pressure and outgassing velocity across the rupture are constant. Once the internal cask pressure drops below the critical lower limit of about 1.9 atm, the pressure and velocity outgassing conditions are assumed to follow Bernoulli's law as well as the ideal gas law.
6.. A total PuO_2 inventory of 0.662 gram is assumed to be present at the start, inside the cask and completely aerosolized into one micron diameter particles. This size is chosen to simulate the worst dose case for an alpha emitter such as PuO2 --- that all the inhaled particles will be respirable.

7. The aerosolized PuO2 particles are emitted at a constant rate during depressurization. They are also assumed to be chemically inert and to have no effect on the surrounding flow field. They are modeled as inert test particles.
8. Particle motion is simulated using Lagrangian tracking methods. Any particle intersecting the ground (bottom, horizontal edges of the near field domain shown in Figure 3 had its tracking terminated and was deemed deposited. Similarly, any particles reaching the right or top edges were terminated as ``escaped", i.e., passed on to the traditional atmospheric transport domain.
9. The wind field prevails after outgassing has stopped. As a result, the wake caused by the cask captures some portion of the released radionuclide aerosols. Such particles are not passed on to the far field (atmospheric transport) domain.
10 . Turbulence effects were modeled using a two equation, standard k-ε model. The model parameter values used in these simulations are:

$C_\mu = 0.09$
$C_{1\varepsilon} = 1.44$
$C_{2\varepsilon} = 1.92$
k Prandtl # = 1.00
ε Prandtl # = 1.30
Energy Prandtl # = 0.85
Wall Prandtl # = 0.85

These parameters specify traits of the k and ε fields necessary for solving their respective transport equations, as described in the ANSYS Fluent theory manual[6].

III. RESULTS FOR A 10^5-ELEMENT MESH

A trustworthy simulation of near field physics even in two dimensions, may influence atmospheric transport through a reduction of pollutant mass that reaches the far field. Reduction was calculated for the four simulations discussed here, and are presented in Table 1. The simulations performed here used Fluent, were fully transient and modeled thermal, momentum, and discrete phase (aerosol) physics. In Fluent, the finite volume method was used, with the values shown in Table 1 obtained using the mesh shown in Figure 2. This mesh is almost entirely made of quadrilaterals, with refinement along the cask surface and in a triangular region extending outward and downward from the one cm cask rupture. The former refinement is needed to capture both the geometry-induced flow separation over the cask and the near-surface pressure values. No boundary layers were directly modeled in these simulations. The triangular refinement region was defined after numerical experiments revealed the expanding, rapidly decelerating outgassing flow to be directed outward and downward (more on this below). It is important to have good spatial resolution of the outgassing jet, as this will dictate the pollutant motion near the cask. Table 1 shows the fractions of the 0:662 gram of aerosolized radionuclide inventory[4] trapped (deposited on the ground), the fraction caught in the wind-created wake after outgassing ends, and the fraction that escapes through the right or top edge of the domain.

Table 1: Wind Wake Capture Of Fractions Of The Aerosolized Radionuclide Inventory

Wind (m/s)	Fraction escaped	Fraction trapped	Fraction caught in wake
0.5	0.60	0.23	0.17
2.0	0.49	0.32	0.19
4.0	0.46	0.23	0.30
6.0	0.43	0.21	0.36
8.0	0.41	0.14	0.45
0.5	0.60	0.23	0.17

In each run the ambient wind field was applied as a velocity inlet condition on the left edge of the domain (Figure 1). At this inlet, velocity is constant in time. As the cask outgassing velocity goes to zero near the end of the simulation, the dominant transport mechanism for material close to the outlet is the cask's bluff-body wake. As this is a recirculation zone, aerosol particles which are still within about one meter of the cask opening will be ``trapped" in this recirculation zone for at least a short time after the velocity of the exiting gas reaches zero. In reality, such particles will not stay trapped forever, mainly because a true wind field is random in time and this randomness will result variously in the diminution, cessation, and re-establishment of the cask's wake. As this was not

modeled, particles within the wake at the end of the simulation were put in a third mass-accounting category, beyond `Escaped' and `Trapped'. The ultimate fate of these particles cannot accurately be determined without inclusion of a stochastic wind field inlet condition.

The mesh shown in Figure 2 is a subdomain of the 23 meter by 7 meter domain and is focused on the cask surface (h=3mm in Figure 3) and the outgassing area (h=5 mm). The global mesh size of Figure 2 is h=7.5 cm. and the full mesh contains about 100,000 elements.

The pressure and normal-velocity curves applied to the inlet-type boundary condition on the one cm. rupture are shown in Figure 3. These are the values obtained from choked flow, Bernoulli's law, and the ideal gas law. Choked flow prevails at the beginning of the outgassing because of the elevated gas pressure and the outgassing geometry.

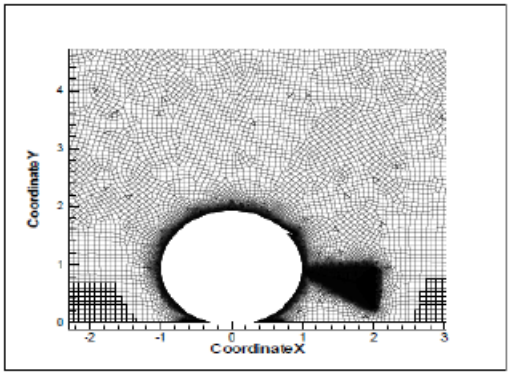

Fig. 2.Mesh used to get the values in Table 1.

The pressure and normal-velocity curves applied to the inlet-type boundary condition on the one cm rupture are shown in Figure 3. These are the values obtained from choked flow, Bernoulli's law, and the ideal gas law. Choked flow prevails at the beginning of the outgassing because of the elevated gas pressure and the outgassing geometry.

Choked flow prevails at the beginning of the outgassing because of both the elevated cask pressure and the outgassing geometry. This geometry is just nozzle flow with an unconstrained expansion into an ambient (1 atm) pressure field at constant temperature (300K). Furthermore, it is reasonable, in developing the BCs for the 1cm rupture outlet, to assume isentropic expansion. This is because no walls constrain the expansion, and walls could yield significant viscous losses.

Temperature equilibration, while occurring over a short distance compared with the scale of the problem domain, nonetheless has a length scale far too large to influence the nozzle-like conditions on the cask rupture surface.

The geometry is nozzle flow with an unconstrained expansion into an ambient pressure field (one atm) at constant temperature (300 ^{o}K). No walls constrain the expansion; walls could yield significant viscous losses. The temperature equilibrates over a distance that is relatively short compared to the problem domain, but the length scale is too large to influence the nozzle-like conditions on the cask rupture surface. The choked temperature T* and pressure p* relative to the values T_0=750K and p_0=2.62 atm inside the cask

$$T^* = T_0\left(\frac{2}{k+1}\right) \qquad (2)$$

$$p^* = p_0\left(\frac{2}{k+1}\right)^{\frac{k}{k-1}} \qquad (3)$$

are[7]

The velocity v* at the one cm rupture inlet is the sonic speed for choked flow

$$v^* = a^* = a_0\left(\frac{2}{k+1}\right)^{1/2} \qquad (4)$$

In order to facilitate reasonable computer run times given a transient time step of dt=2x10^{-4} sec, the time shown in Figure 4 is the actual mechanical equilibration time compressed by a factor of 500. Thus, the outgassing velocity reached zero at simulation time t_{sim}=3.894 sec. This time compression is acceptable because none of the important physical processes (particle motion, choked and ideal gas outgassing) require a longer time scale than was used in the simulations. Furthermore, with a time step of approximately 2x10^{-4} seconds, the average CFL number for the cells through which the outgassing flow passes is about 7[9]. This value is obtained using a mean velocity of about 100 meters/sec – slightly more than the actual value because of the rapid deceleration from 284 meters/sec at the outlet to about 15 meters/sec near the ground. For such a rapidly decelerating flow, using a semi-implicit time stepping method, and given that the near sonic flow behavior very close to the cask slit is of little interest, such a CFL number is acceptable.

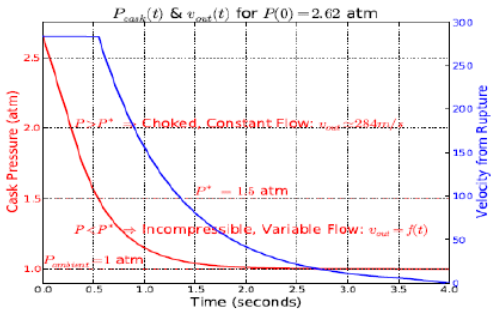

Fig. 3. Pressure and velocity boundary conditions applied to the one cm cask rupture.

After the cask reaches pressure equilibrium with the surroundings (t_{sim}=3.894sec), the simulations were continued for several more seconds so that all particles downwind of the wake would have time to deposit on the ground or reach the end of the domain. Typically, this was about 10 seconds of simulation time.

Buoyancy forces are driven by local changes in density caused by locally elevated temperatures. Such forces are small in comparison to the pressure gradients which drive flows in the absence of thermal considerations. Thus in these simulations, the flow field, and hence the pollutant motion, is almost entirely determined by the pressure changes in the problem domain. There are two ``flow regimes" over the course of the simulation time. The first prevails early on when the outgassing velocity is still very large relative to the ambient wind speed ($v_{out} >> v_{amb}$), and the second when the two are about the same order of magnitude. The simulation is studied with wind speed v_{amb}= 2 meters/sec. Figure 5 shows the aerosol particle number density at t_{sim}=0.6 sec as well as the pressure field near the cask. At this early time, the outgassing flow is still choked ($v_{out}=v^*$= 284m/sec) and the high-speed flow causes a region of low pressure to develop below the outgassing stream. This low pressure value is denoted as ``p_{ptcl}" since it is associated with the particle flow near the cask; the low pressure value at the top of the cask that is associated with Bernoulli--type acceleration is denoted by "p_{cask}".

Figure 4 shows that the wake set up by the low pressure is underneath the particle stream, so that most particles emitted at about this time move downward and outward, either depositing on the ground or moving out of the domain. The typical bluff--body wake that would prevail without the cask rupture has collapsed under the influence of the much lower pressure set up by the outgassing flow (ppart). The result, seen in the stream traces in Figure 6, is that the particle paths follow a sharply defined arc starting at the rupture and continuing to just above the ground, at which point the particles have slowed considerably. This deceleration of the outgassing jet generates a small region of high pressure, which is shown as the red region close to the ground. The details of this motion are not well resolved because this high pressure region falls outside the triangular refinement area of the mesh, The second flow regime, in which v_{out} is not much larger than v_{amb}, prevails from near the end of outgassing (t_{sim} > 3.0 seconds) until the end of the simulation. In this regime, p_{cask} and p_{ptcl} are about the same order of magnitude. Early in this regime, the particle flow is pulled upward under the now important influence of p_{cask}, as shown in Figure 5. The particle stream approaches the ground, moving from the downwind direction and curling back towards the cask along the ground.

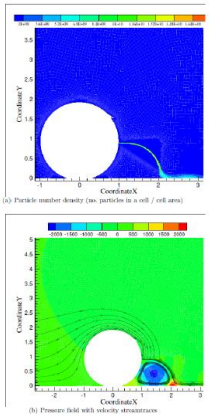

Fig.4. Illustration of the first flow regimen studied. Parameters are v_{amb}=2meters/sec, t_{sim}=0.6 seconds, $p_{part} << p_{cask}$

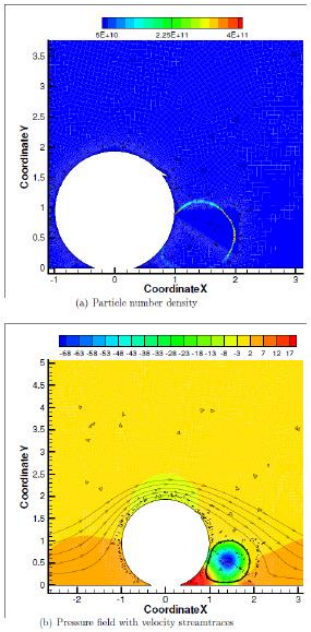

Fig. 5. This figure shows the early stages of the second flow regime, in which p_{ptcl} is not much larger than p_{cask}.. Distances are in meters**.**

From approximately t_{sim}=3.5 seconds until the end of the outgassing (3.984 seconds),the particle stream is increasingly pulled upward because of the low pressure at the top of the cask. During the second flow regime, most of the particles escaping from the cask will be trapped by the cask's bluff-body wake. That wake is re-established because p_{ptcl} gradually merges with p_{cask}. Figure 6 shows stream traces and particle counts for t_{sim}=5 seconds, after outgassing has stopped. The particles in the cask's wake are caught there for the rest of the simulation, since the wake remains quasi-steady.

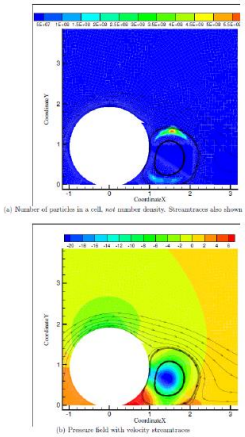

Fig. 6. Illustration of the second flow regime.

By t_{sim}= 5.0 seconds, the cask internal pressure has equilibrated with ambient atmosphere atmospheric pressure, and outgassing has stopped. The particles shown in Figure 8 are caught in the bluff-body cask wake for the remainder of the simulation. A remnant of the low pressure region formed during outgassing are still present but are substantially weaker: $p_{ptcl} \approx$ -22 Pa (2x10^{-4} atm) and $p_{cask} \approx$ -8 Pa (8x10^{-5} atm). Figure 8 of the simulation time with 2 meter/second wind. The figure also shows the outgassing velocity v_{out},, from which it is apparent that as v_{out} goes to zero, p_{ptcl} goes to p_{cask}. Early in the simulation $p_{ptcl}/ p_{cask} \approx 65$, while for $t_{sim} > 3.0$ seconds, $p_{ptcl}/ p_{cask} < 12$. Thus v_{out} appears to determine which flow regime prevails.

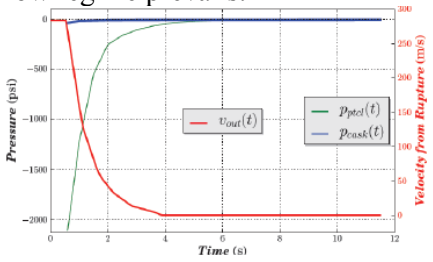

Fig' 7. Change in p_{ptcl} and p_{cask} with change in v_{out}..

IV. Results for Refined Mesh

In order to more accurately resolve the particle jet near the ground more accurately during the first flow regime, a mesh similar to that shown in Figure 3 but with a larger triangular refinement area is used. Figure 8 shows a close-up view of the enlarged refinement zone. The larger refinement area shown in Figure 8 captures the motion of particles near the ground more accurately. The resolution of the particle flow near the ground is the source of the different particle outcomes between corresponding simulations on the two meshes. This particle flow resolution is dramatic, and is shown in Figure 9.

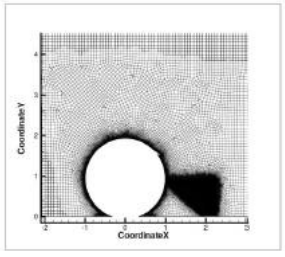

Fig.8. Mesh using a larger refinement area around the outgassing jet.(distance in meters)

Figure 9 shows a striking difference in resolution of the near-ground particle motion. With greater spatial resolution where the outgassing jet nears the ground, the more refined mesh of Figure 9(b) is able to capture a pronounced outward turn (parallel to the ground) of the particles which is unresolved in Figure 9(a). This outward turn leads to a smaller portion of the released aerosol being deposited on the ground, and a larger fraction escaping into the far field domain.

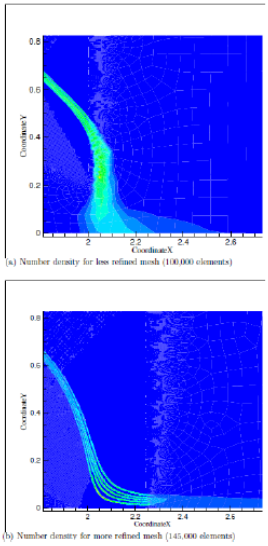

Figure 9. Influence of mesh refinement on resolution of the near-ground particle motion (distance in meters.

The mass fractions shown in Table 1 were computed for the more refined mesh, and are shown in Table 2. The most important mass fraction is that which escapes to the far field. These values are plotted against wind speed in Figure 10.

Table 2: Wind Wake Capture Of Fractions Of The Aerosolized Radionuclide Inventory

Wind (m/s)	Fraction escaped	Fraction trapped	Fraction caught in wake
0.5	0.30	0.50	0.20
2.0	0.26	0.50	0.24
4.0	0.17	0.52	0.31
6.0	0.16	0.41	0.43
8.0	0.13	0.37	0.5

The fraction of the 0.662 gram radionuclide inventory which is advected to the far field as a function of wind speed. The fractions are cited in the Fraction Escaped column of Table 2. In comparison with the values in Table 1, obtained using a mesh with a smaller outgassing refinement area, the fraction of the pollutant inventory escaping to the far field has roughly doubled in the worst case and more than tripled in the best case of (v_{amb}=8.0 meters/second. The motion of the particles near the ground can be captured more accurately by using a larger refinement area around the outgassing jet. On the less refined mesh of Figure 2, the particles do not exhibit the sharp outward turn seen on the more refined mesh.

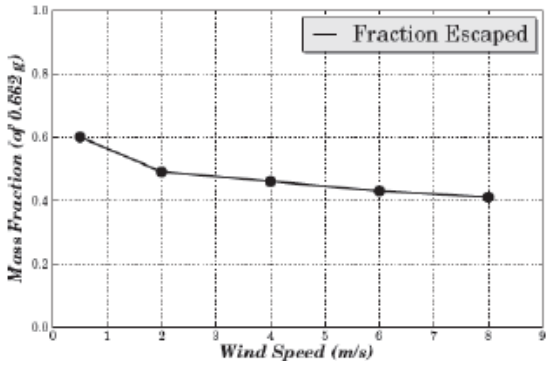

Fig. 10. Fraction of the radionuclide inventory advected to the far field

The results presented assume the rupture emits radionuclide aerosols at a constant rate rather than at a rate which reflects the instantaneous state of cask depressurization. This approach is taken in order to have correct particle flow calculations over the areas of high mesh refinement, without the necessity of taking a prohibitively small time step.

By focusing exclusively on each of the two flow regimes, precise estimates of the particle outcomes in each regime (i.e. escaped, deposited, and caught in the cask wake) are possible. It appears that most pollutant mass will be emitted during the first flow regime. In fact, numerical integration of v_{out} (t) gives a value of 0.963, which leaves 0.037 of the mass to be emitted during the second flow regime. By weighting the mass fractions of particle outcomes using these two values we may ``reassemble" a better approximation to the rate of change in released mass as a function of the outgassing speed, with the following results for v_{amb}=2 meters/second:

Escaped fraction = 0.757
Trapped (deposited) fraction = 0.228
Fraction caught in wake = 0.015

A more physically realistic mass accounting, using the more accurate mesh of Figure 9, yield show three-quarters of the radionuclide inventory advected out to the traditional far field domain. Using a factor of 0.757/0.49 taken from the above results and Table 2 as a guide to extending the results of the `Escaped' column in Table 2, in the st case that most pollutant passes onto the far field, v_{amb} =0.5 meters/second, 92.7 percent is advected out of the near field.

Calculating a two-dimensional transient pollutant concentration field involves the effect of a crosswind perpendicular to the cask's long axis, buoyancy of the radionuclide flow caused by decay-heat induced high temperatures inside the cask, and tracking the radionuclide aerosols so concentrations can be calculated.

The wind perpendicular to the cylindrical package axis has a potentially large impact on the concentration field. On its own, the wind field is expected to develop into a roughly steady state shape with stagnation at the left-most point on the cask's upwind side and a recirculating wake field on the downwind side. If buoyancy effects are included, the problem becomes fully transient. If the rupture (where the aerosolized radionuclides are emitted) is facing into the recirculation zone, much of concentration field may be localized in this zone. However, if the rupture is perpendicular to the wind or slightly into the wind, the aerosol may follow streamlines near, but above the recirculation zone, enabling them to travel farther downstream. In either case, the wind around the cask will strongly influence the near-rupture buoyancy driven flow**.**

V. Results and Conclusions To Date

As the figures show, the plume of released material cools rather quickly to the ambient temperature, and then is lofted slowly by its buoyancy. However, immediately after release, while the temperature of the released plume is higher than that of the ambient wind, the plume appears to be trapped in the downwash on the downwind side of the cask. If the plume contains any particulate material, that material appears to be trapped temporarily in the downwash and might be deposited, depleting the particulate plume. RADTRAN analysts usually assign a somewhat arbitrary terminal velocity of 0.01 meters per second to particulate matter. Since the plume is released at a height of about one meter in this model, activity could deposit out of the plume and any person standing next to the cask would sustain an external dose. As the plume rises it potentially contributes to air that is inhaled by nearby persons, delivering an inhalation dose. Contributions to the near field occupational dose are from both deposited and inhaled material. In addition, any depletion of the plume in the near field results in decreased activity n the far field which is modeled using Gaussian dispersion.

REFERENCES

1. NRC (Nuclear Regulatory Commission), 1977, “Final Environmental Statement on the Transportation of Radioactive Materials by Air and other Modes,” NUREG-0170, Nuclear Regulatory Commission, Washington DC
2. U. S. Code of Federal Regulations, Volume 10, Section 71.73.
3. Hunt, J.C.R. 1985. Turbulent Diffusion from Sources in Complex Flows. *Ann. Rev. Fluid Mech.* 1985, v. 17, pp. 447-85.
4. NRC (Nuclear Regulatory Commission), 2014, “Spent Fuel Transportation Risk Assessment” NUREG-2125, Nuclear Regulatory Commission, Washington DC
5. Turner, D.B., *Workbook of Atmospheric Dispersion Estimates*, Lewis Publishers, New York, NY, 1994
6. ANSYS Inc. ANSYS Fluent Ver 15.0.0. http://www.ansys.com/Products. 2013
7. Faires, V.M. and Simmang, C.M. *Fundamentals of Atmospheric Modeling*, Macmillan, New York, 1978.